*Inorg. Chem.* **2006**, *45*, 1693–1697

# Nanoscale Zinc Antimonides: Synthesis and Phase Stability

**Sabine Schlecht,* Christoph Erk, and Maekele Yosef**

*Freie Universität Berlin, Institut für Chemie und Biochemie, 14195 Berlin, Germany*

Received October 19, 2005

Highly crystalline single-phase nanoparticles of the important thermoelectric materials $Zn_4Sb_3$ and ZnSb were prepared from solvochemically activated powders of elemental zinc and elemental antimony. Low-temperature reactions with reaction temperatures of 275–300 °C were applied using an excess of elemental zinc. The nanoscale thermoelectrics obtained were characterized by X-ray powder diffraction, transmission electron microscopy, and thermal analysis. nc-$Zn_4Sb_3$ showed particle sizes of 50–70 nm, whereas particle sizes of 15–20 nm were observed for nc-ZnSb. Calorimetric investigations showed an increased heat capacity, $C_p$, for nc-$Zn_4Sb_3$ with respect to the bulk material which could be reduced to the bulk value by annealing nc-$Zn_4Sb_3$ at 190 °C. Interestingly, nc-$Zn_4Sb_3$ showed exothermic decomposition into zinc-poorer ZnSn at 196 °C in an open system, indicating that $Zn_4Sb_3$ is metastable in nanocrystalline form at room temperature.

## Introduction

The conversion of heat into electrical energy and vice versa represents one of the future key challenges in technology. Thus, the improvement of high-performance thermoelectric materials for solid-state refrigerators or for the generation of electrical energy in space, for example, is of major importance.[1,2] Among the best thermoelectric materials known to date are the zinc antimonides $Zn_4Sb_3$ and ZnSb which are especially effective between 150 and 400 °C. At a temperature of 400 °C, $Zn_4Sb_3$ has the highest figure of merit, ZT ≈ 1.3, of all known binary thermoelectrics.[3] The figure of merit of a thermoelectric material is defined by $ZT = (\alpha^2\sigma/\kappa)T$, where $\sigma$ is the electrical conductivity, $\kappa$ is the thermal conductivity, and $\alpha$ is the Seebeck coefficient of the respective material. The thermoelectrical power factor, $\alpha^2\sigma$, of $Zn_4Sb_3$ is not especially high, and the exceptional figure of merit of this compound stems from a particularly low thermal conductivity of $\sim 6 \times 10^{-3}$ W cm$^{-1}$ K$^{-1}$ for this zinc antimonide in the temperature range of 200−400 °C.[3] A significant body of work was published recently to elucidate the structural origins of this very low value.[3−6] Disordered interstitial zinc atoms and the corresponding vacancies seem to be the predominant features leading to very efficient phonon scattering and thus to a very low thermal conductivity.[3,4] This structural motif has also been found for the more zinc-rich $\zeta$-$Zn_{3-x}Sb_2$ phase,[7] but it is not present in ZnSb which consequently shows a much higher thermal conductivity than $Zn_4Sb_3$.[3] The important role of interstitials as "rattlers" in the voids of a structure has been pointed out in the "phonon-glass-electron-crystal" model by Slack.[8]

One major general concept for lowering the thermal conductivity is the application of low-dimension materials such as nanoscale particles or wires that provide effective phonon scattering at a large number of grain boundaries.[9] Prominent examples of this concept are the nanoscale superlattice structures of thin films of $Bi_2Te_3/Sb_2Te_3$,[10] PbTe/$Pb_{1-x}Eu_xTe$,[11a] or PbSeTe/PbTe[11b] and nanocomposite phases such as $AgPb_mSbTe_{2+m}$[12] with very high figures of merit.

* To whom correspondence should be addressed. E-mail: schlecht@chemie.fu-berlin.de. Fax: +49-(0)30-838-53310.

(1) Nolas, G. S.; Sharp, J.; Goldsmid, H. J. *Thermoelectrics: Basic Principles and New Materials Developments*; Springer: Berlin, 2001.
(2) (a) DiSalvo, F. J. *Science* **1999**, *285*, 703. (b) Tritt, T. M. *Science* **1999**, *283*, 804.
(3) (a) Snyder, G. J.; Christensen, M.; Nishibori, E.; Caillat, T.; Iversen, B. B. *Nature Mater.* **2004**, *3*, 458. (b) Caillat, T.; Fleurial, J. P.; Borshchevsky, A. *J. Phys. Chem. Solids* **1997**, *58*, 1119.
(4) Cargnoni, F.; Nishibori, E.; Rabiller, P.; Bertini, L.; Snyder, G. J.; Christensen, M.; Gatti, C.; Iversen, B. B. *Chem.—Eur. J.* **2004**, *10*, 3861.
(5) Nylén, J.; Andersson, M.; Lidin, S.; Häussermann, U. *J. Am. Chem. Soc.* **2004**, *126*, 16306.
(6) Mozharivskyj, Y.; Pecharsky, A. O.; Bud'ko, S.; Miller, G. J. *Chem. Mater.* **2004**, *16*, 1580.
(7) Boström, M.; Lidin, S. *J. Alloys Compd.* **2004**, *376*, 49.
(8) Slack, G. A. In *CRC Handbook of Thermoelectrics*; Rowe, D. M., Ed.; CRC Press: Boca Raton, FL, 1995; p 407.
(9) (a) Casimir, H. B. G. *Physica* **1938**, *5*, 495. (b) Hicks, L. D.; Dresselhaus, M. S. *Phys. Rev. B.* **1993**, *47*, 12727. (c) Hicks, L. D.; Dresselhaus, M. S. *Phys. Rev. B.* **1993**, *47*, 16631.
(10) (a) Venkatasubramanian, R.; Colpitts, T.; O'Quinn, B.; Liu, S.; El-Masry, N.; Lamvik, M. *Appl. Phys. Lett.* **1999**, *75*, 1104. (b) Venkatasubramanian, R.; Siivola, E.; Colpitts, T.; O'Quinn, B. *Nature* **2001**, *413*, 597.

10.1021/ic051808t CCC: $33.50 
Published on Web 01/10/2006

Here, we present an extension of the concept of nanoscale thermoelectrics on the zinc antimonides $Zn_4Sb_3$ and ZnSb. Because of the intrinsically metastable nature of nanoscale matter, a low-temperature synthetic route to ZnSb and $Zn_4Sb_3$ had to be applied. A simple and versatile approach to nanoscale binary intermetallic compounds is the reaction of the two required elements in activated (i.e., finely dispersed) form[13] leading to nanoparticles of the binary compound. The small particle size of the reactands ensures minimum diffusion paths, low activation barriers, and low reaction temperatures.

## Results and Discussion

The synthesis of nanoparticles of $Zn_4Sb_3$ and ZnSb was achieved through the reaction of activated zinc with activated antimony in the temperature region of 275−300 °C. The reactands were produced by reduction of solutions of $ZnCl_2$ and $SbCl_3$ in tetrahydrofuran with a solution of lithium triethylboronhydride $Li[Et_3BH]$ in tetrahydrofuran. The exact reaction conditions are given in eqs 1 and 2.

$$ZnCl_2 + 2Li[Et_3BH] \xrightarrow[\text{reflux, 2 h}]{\text{THF}} Zn^* + H_2 + 2BEt_3 + 2LiCl \quad (1)$$

$$SbCl_3 + 3Li[Et_3BH] \xrightarrow[\text{rt, 30 min}]{\text{THF}} Sb^* + 1.5H_2 + 3BEt_3 + 3LiCl \quad (2)$$

The metal powders obtained were washed repeatedly with dry tetrahydrofuran to remove residual lithium salts and were subsequently dried under vacuum. The activated elements were placed in a Schlenk ampule and heated in an electrical furnace under argon. The reactions were conducted with an excess of zinc metal which was removed by a short treatment with dilute acetic acid after the reaction was completed. For the preparation of the $Zn_4Sb_3$ nanoparticles, an ampule filled with the activated elements in a molar ratio between 2.5:1 and 3:1 (Zn/Sb) was heated to 300 °C at a rate of 15 K/min and immediately cooled to 275 °C after this temperature was reached. The reaction temperature was held at 275 °C for 15 h; then the reaction mixture was allowed to cool to room temperature. The product was collected and stirred in 2% acetic acid at room temperature for 5−10 min, depending on the overall amount of material. The lowering of the reaction temperature from 300 to 275 °C turned out to be crucial for the synthesis of nanocrystalline $Zn_4Sb_3$. When the reaction temperature is held at more than 285 °C, the nanocrystalline $Zn_4Sb_3$ decomposes into nanocrystalline ZnSb with loss of elemental zinc. Hence, nanoparticles of ZnSb are obtained when the reaction is held at 300 °C for 15 h. Overview TEM micrographs and high-resolution TEM images of as-obtained nanoparticles of $Zn_4Sb_3$ and ZnSb, after the elemental zinc was removed, were taken to investigate particle sizes and crystallinity. In the case of $Zn_4Sb_3$, particles without facets of 50−70 nm in size were produced (Figure 1), whereas the ZnSb particles were only about 15−20 nm in size and were also rather featureless (Figure 2). HRTEM images of nanoparticles of both phases show the good crystallinity of the nanoscale material (Figures 1 and 2). This is confirmed by the X-ray powder diffraction patterns of $Zn_4Sb_3$ and ZnSb (Figure 3). The XRD patterns could be indexed on the basis of bulk orthorhombic ZnSb (space group *Pbca*) and rhombohedral $Zn_4Sb_3$ (space group $R\bar{3}c$).[6] As the reflections of the rather big particles of $Zn_4Sb_3$ show only marginal broadening, an estimation of the grain size according to Scherrer's equation[14] was only done for ZnSb. A particle size of 18 ± 2 nm was obtained, which is in good agreement with the geometrical particle size found on the TEM images.

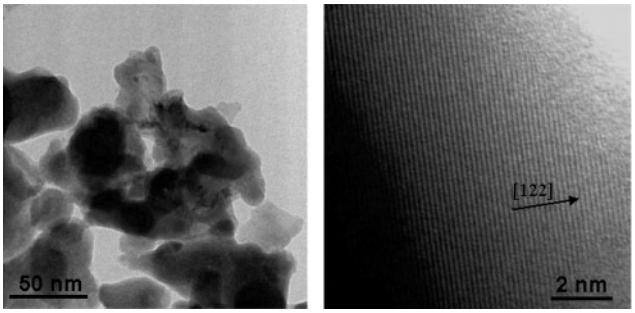


**Figure 1.** TEM overview micrograph of nanoparticles of $Zn_4Sb_3$ (left) and an HRTEM image of a single nanoparticle showing {122} lattice fringes (right).

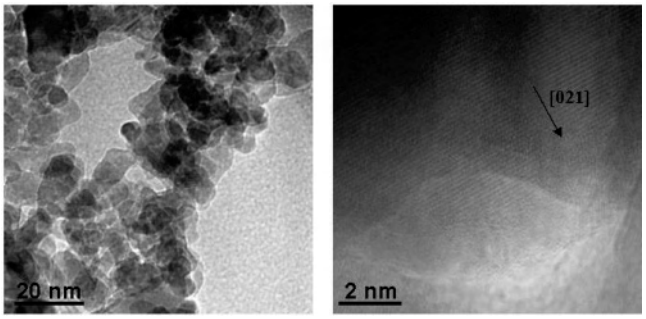


**Figure 2.** TEM overview micrograph of nanoparticles of ZnSb (left) and an HRTEM image of a single nanoparticle showing {021} lattice fringes (right).

The thermal lability of the $Zn_4Sb_3$ particles during the process of preparation is striking and does not correspond to the thermal stability of this phase in the bulk according to the phase diagram where a decomposition temperature of 492 °C is denoted;[15] however, a certain tendency to lose elemental zinc at a fairly low temperature had already been observed for bulk $Zn_4Sb_3$ earlier. In these experiments, bulk $Zn_4Sb_3$ was heated under vacuum and significant decomposition into ZnSb and Zn started around 290 °C.[6] We heated

(11) (a) Harman, T. C.; Spears, D. L.; Manfra, M. J. *J. Electron. Mater*. **1996**, *25*, 1121. (b) Harman, T. C.; Taylor, P. J.; Walsh, M. P.; LaForge, B. E. *Science* **2002**, *297*, 2229.
(12) (a) Hsu, K. F.; Loo, S.; Guo, F.; Chen, W.; Dyck, J. S.; Uher, C.; Hogan, T.; Polychroniadis, E. K.; Kanatzidis, M. G. *Science* **2004**, *303*, 818. (b) Quarez, E.; Hsu, K. F.; Pcionek, R.; Frangis, N.; Polychroniadis, E. K.; Kanatzidis, M. G. *J. Am. Chem. Soc*. **2005**, *127*, 9177.
(13) Bönnemann, H.; Brijoux, W. Catalytically Active Metal Powders. In *Active Metals*; Fürstner, A., Ed.; VCH: Weinheim, Germany, 1996; pp 339−379.
(14) Guinier, A. *X-ray Diffraction in Crystals, Imperfect Crystals and Amorphous Bodies*; Dover: New York, 1994; pp 121−130.
(15) Massalski, T. E., Ed. *Binary Alloy Phase Diagrams*; ASM International: Materials Park, OH, 1990.

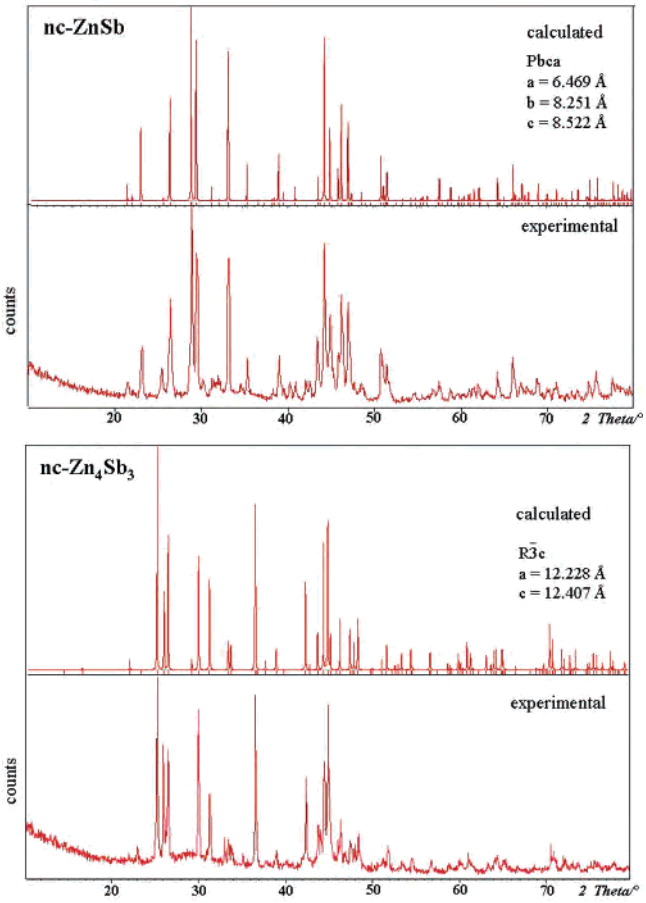


**Figure 3.** Experimental and calculated X-ray powder diffraction patterns of nc-ZnSb (top) and nc-$Zn_4Sb_3$ (bottom).

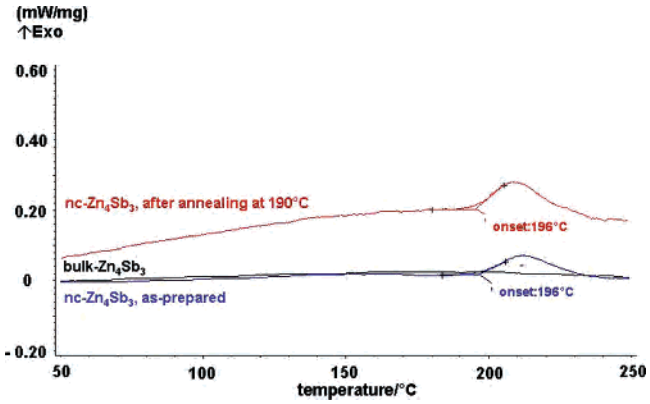


**Figure 4.** DSC curves in the temperature range of 50−250 °C for bulk-$Zn_4Sb_3$, as-prepared nc-$Zn_4Sb_3$, and annealed nc-$Zn_4Sb_3$. Both nc-$Zn_4Sb_3$ samples show an exothermic decomposition event with an onset temperature of 196 °C (the different shape of the curve for annealed nc-$Zn_4Sb_3$ results from the use of a different set of pans).

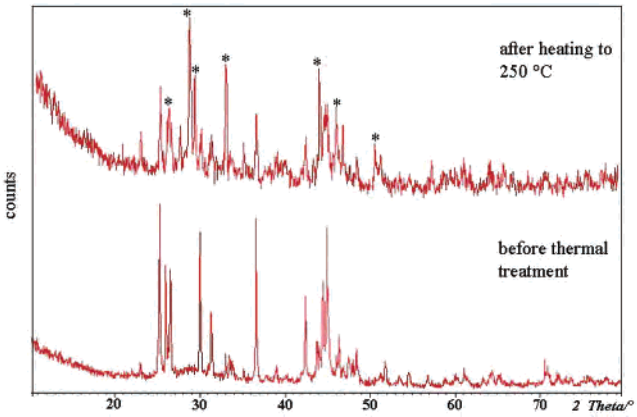


**Figure 5.** X-ray powder diffraction pattern of nc-$Zn_4Sb_3$ before and after the decomposition step at 196 °C. Dominant reflections of the ZnSb phase formed in the decomposition are marked with an asterisk.

samples of bulk $Zn_4Sb_3$ in an argon atmosphere at ambient pressure and observed a continuous slow decomposition starting at 300 °C. This decomposition process seems to be much more favorable for nanoscale $Zn_4Sb_3$, and we observed decomposition starting at 280 °C under the preparation conditions (i.e., in the presence of an excess of zinc metal under normal pressure (eq 3)).

$$\text{nc-}Zn_4Sb_3 + \text{excess Zn} \xrightarrow{280\ ^\circ\text{C}} 3\text{nc-ZnSb} + \text{excess Zn} \quad (3a)$$

$$\text{nc-}Zn_4Sb_3 \xrightarrow{200\ ^\circ\text{C}} 3\text{nc-ZnSb} + \text{Zn} \quad (3b)$$

Aiming at a further elucidation of these decomposition phenomena, we conducted calorimetric measurements with nanocrystalline $Zn_4Sb_3$ in the absence of additional zinc. The heating of pure nc-$Zn_4Sb_3$ to 250 °C revealed an exothermic event with an onset temperature of 196 °C (Figure 4). An XRD pattern of this sample was recorded after the DSC experiment which showed that most of the $Zn_4Sb_3$ had decomposed during this exothermic transformation (Figure 5). When a sample of nc-$Zn_4Sb_3$ was subjected to a temperature of 250 °C for 1 h, decomposition almost reached completion. In an additional DSC experiment, we heated a sample of nc-$Zn_4Sb_3$ to 190 °C (e.g., slightly below the decomposition temperature), held this temperature for 1 h, cooled the sample down to room temperature, and looked at its decomposition characteristics again. Although a certain degree of annealing was achieved by this procedure, the onset temperature for the decomposition remained unchanged at 196 °C (Figure 4), and no improvement of the thermal stability was observed.

Several possible reasons for the thermal instability of nanocrystalline $Zn_4Sb_3$ can be imagined. The decomposition could originate from a strong increase of the vapor pressure of zinc in the nanoscale material or from a significant increase of the surface energy of nc-$Zn_4Sb_3$ compared to the bulk material that is much more pronounced for $Zn_4Sb_3$ nanoparticles than for nanoscale ZnSb. Another factor of thermal instability could be a significantly higher uptake of thermal energy in the case of the particles. Thus, we measured the heat capacities, $C_p$, of nc-ZnSb, bulk $Zn_4Sb_3$, pure nc-$Zn_4Sb_3$ (named as-prepared nc-$Zn_4Sb_3$ in the following), and pure nc-$Zn_4Sb_3$ which was previously annealed at 190 °C for 1 h in the temperature range of 50−90 °C. This low-temperature region was chosen to avoid sintering and particle growth during the measurements. Whereas nc-ZnSb shows $C_p$ values only slightly higher than the expected bulk value of $3R = 24.9$ J mol$^{-1}$ K$^{-1}$ for ZnSb, all $Zn_4Sb_3$ samples show $C_p$ values higher than the Dulong−Petit limit, reflecting the "phonon-glass-type" characteristics of this compound (Figure 6). In comparison to the heat capacities

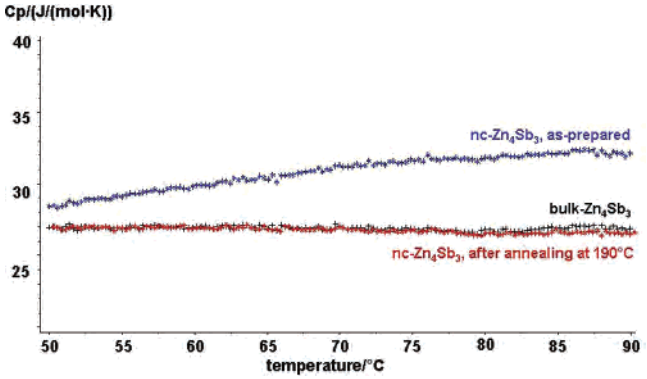


**Figure 6.** Heat capacities, $C_p$, of bulk-$Zn_4Sb_3$, as-prepared nc-$Zn_4Sb_3$, and annealed nc-$Zn_4Sb_3$ in the temperature range of 50−90 °C.

of the $Zn_4Sb_3$ samples, the $C_p$ values of the nanocrystalline sample are again higher than the value of the bulk material. This tendency is generally observed for a number of nanoscale materials, and the enhancement of the heat capacities can vary from 1−2% (for $Ni_{80}P_{20}$ and selenium)[16] to 48% (for palladium).[17] For the as-prepared nc-$Zn_4Sb_3$, the enhancement is about 12% on average in the temperature range measured here. Interestingly, the heat capacity of nc-$Zn_4Sb_3$ dropped to the bulk value when the sample was annealed at 190 °C for only 1 h (Figure 6). Thus, the enhancement of the $C_p$ value of the as-prepared nanoparticles, normally attributed to a higher-than-average contribution from surface lattice vibrations,[17−19] can be eliminated by moderate thermal treatment in the case of $Zn_4Sb_3$. The annealing seems to heal certain defects and surface states which were created either during the synthesis or with the removal of elemental zinc. The decrease in the heat capacity of the annealed sample did not influence the decomposition temperature and thermal stability of the material (Figure 4). Hence, the higher uptake of thermal energy by the nanoparticles of $Zn_4Sb_3$ cannot be correlated with their decomposition characteristics. In addition to an expected increase of the zinc vapor pressure for nanoscale particles of $Zn_4Sb_3$ and an increased surface energy, a higher volume enthalpy content of the nanocrystals caused by subtle structural differences and defects in nanoscale $Zn_4Sb_3$ might account for the low-temperature decomposition of these particles leading to ZnSb.

The key result of the investigations of the thermal properties of nanoscale ZnSb and $Zn_4Sb_3$ is the decomposition of nc-$Zn_4Sb_3$ below 200 °C with substantial consequences for possible applications of nanoscale $Zn_4Sb_3$ as a thermoelectric material. The desired temperature range with an excellent figure of merit for this compound is between 200 and 400 °C, but these temperatures are not tolerated by nc-$Zn_4Sb_3$ when it is heated in an open system. The peculiar structural features of $Zn_4Sb_3$, namely, the presence of interstitial zinc atoms and an only partially occupied zinc site leading to a significant degree of intrinsic disorder,[4] a very low thermal conductivity, and superior thermoelectric properties also seem to be responsible for the thermal collapse of this phase on the nanoscale. The interstitial zinc atoms in the structure of $Zn_4Sb_3$ are especially mobile and can easily migrate to the particle surface where enhanced lattice dynamics will facilitate the transformation into ZnSb under zinc loss. The, generally, further reduced kinetic barrier for the transformation of $Zn_4Sb_3$ into ZnSb in small particles facilitates the decomposition of nc-$Zn_4Sb_3$, which is a metastable phase at low temperatures when nanocrystalline.

## Summary

The use of nanoscale powders of activated zinc and antimony allowed the low-temperature synthesis of nanoparticles of the binary thermoelectrics ZnSb and $Zn_4Sb_3$. The as-obtained products were highly crystalline single-phase materials. Thermal investigation of nc-ZnSb and nc-$Zn_4Sb_3$ revealed an enhanced heat capacity for nc-$Zn_4Sb_3$ which could be reduced to the bulk value of $Zn_4Sb_3$ by annealing at 190 °C. A finding of substantial significance for possible future applications is the thermal decomposition of nanoscale $Zn_4Sb_3$ below 200 °C in an open system.

## Experimental Section

**Synthetic Procedures.** Tetrahydrofuran was dried over sodium and freshly distilled before use. Zinc chloride was dried with thionyl chloride, washed with toluene, and dried under a vacuum before use. Lithium triethylboronhydride (Aldrich, 1 M in THF) and antimony(III) chloride were used as obtained. Activated antimony was obtained in a room-temperature reaction of a solution of $SbCl_3$ in tetrahydrofuran with 3 equiv of a 1 M solution of lithium triethylboronhydride for 30 min. Activated zinc was produced by the reaction of a solution of $ZnCl_2$ in tetrahydrofuran with 2 equiv of a 1 M solution of lithium triethylboronhydride at 65 °C for 2 h. Activated zinc powder and activated antimony powder were washed several times with tetrahydrofuran after the initial reaction solution was decanted. The washed products were dried in a vacuum. The antimonides were prepared in long Schlenk ampules with a pressure valve attached to the top. The preparation of nanoparticles of $Zn_4Sb_3$ and ZnSb was conducted with a 3:1 excess of zinc powder. The residual excess zinc was removed after the reaction by a 10 min treatment with a 2% acetic acid solution and subsequent washing of the remaining zinc antimonide with deionized water until neutrality was reached.

**Calorimetric Measurements.** Thermal analyses were carried out under a dynamic argon atmosphere using a Netzsch Pegasus 404 DSC calorimeter. Thirty milligrams of ZnSb, $Zn_4Sb_3$, nc-ZnSb, or nc-$Zn_4Sb_3$ was placed in a double-wall DSC pan consisting of a Pt/Rh mantle and an $Al_2O_3$ inlay, covered with a Pt/Rh lid. The calorimeter was evacuated twice and filled with argon before the measurements. The measurements were carried out under a constant gentle flow of argon at a heating rate of 10 K/min. $C_p$ measurements were calibrated on a sample of elemental silver, the heat capacity of which was given in ref 20. $C_p$ values are given for an average atom equivalent of the molar heat capacity, namely, $1/7C_p$-($Zn_4Sb_3$).

**Electron Microscopy.** Transmission electron microscopy was performed using a JEOL JEM 3010 electron microscope (300 kV, $LaB_6$ cathode). The samples were finely dispersed in ethanol. One drop of the dispersion was placed on a carbon-coated copper grid

(16) Sun, N. X.; Lu, K. *Phys. Rev. B* **1996**, *54*, 6058.
(17) Rupp, J.; Birringer, R. *Phys. Rev. B* **1987**, *36*, 7888.
(18) Bai, H. Y.; Luo, J. L.; Jin, D.; Sun, J. R. *J. Appl. Phys.* **1996**, *79*, 361.
(19) Novotny, V.; Meincke, P. P. M. *Phys. Rev. B* **1973**, *8*, 4186.
(20) Moser, H. *Physik. Z.* **1936**, *37*, 737.

and allowed to dry, leaving the crystallites in a random orientation on the support film.

**Acknowledgment.** We thank Prof. Dr. Bernd Harbrecht and Samuel Freistein (Philipps-Universität Marburg) for providing a sample of bulk $Zn_4Sb_3$. Financial support by the Deutsche Forschungsgemeinschaft and the Fonds der Chemischen Industrie is gratefully acknowledged.

IC051808T